



# CFD Modeling of Melt Spreading Behavior on Spinning Discs and Cups for Centrifugal Granulation of Molten Slag

Yuhua Pan<sup>1</sup> · Ming Zhao<sup>1</sup> · Ping Ma<sup>1</sup> · Jing Li<sup>1</sup> · Zhaoyi Huo<sup>1</sup> · Hongyu Li<sup>1</sup>

Published online: 8 February 2019  
© The Minerals, Metals & Materials Society 2019

## Abstract

The spreading behaviors of molten slag on spinning discs and cups were studied through performing free surface flow numerical simulations by means of computational fluid dynamics (CFD) modeling technique. In this work, liquid slag film thickness at the edge of the spinning discs and cups was predicted by using the CFD model, since the slag film thickness has a predominant influence on the size of the slag granules produced after the slag film breakup. The effects of the shape of discs and cups and the operating conditions (slag flowrate and spinning speed) on the slag film thickness were examined. Flat surface disc, disc with curved surface, and cups with different sidewall height and taper angle were investigated. It was found from the modeling results that, under the same slag flowrate and spinning speed, the larger the wetting area of the slag on the discs and cups, the smaller the slag film thickness. For the same size (radius) discs and cups, the slag film thickness on the flat surface disc is larger than those on the cup and the curved surface disc. Furthermore, the film thickness on the cup is larger than that on the curved surface disc. The reason is that the cup has a sharp corner and a sidewall that impose a larger resistance to the slag flow, whereas the curved surface disc has a smooth surface that has a smaller resistance to the slag flow.

**Keywords** Centrifugal granulation · Spinning disc · Spinning cup · Molten slag · Film thickness · Free surface flow

## Nomenclature

### Alphabetic Symbols

$C_\mu$	Constant in turbulence model
$\mathbf{F}$	Body force vector
$F_1$	First blending function in turbulence model
$H$	Depth of curved surface disc and cup
$k$	Turbulence kinetic energy
$N_p$	Total number of fluid phases ( $N_p = 2$ for liquid slag and air)
$p$	Pressure
$P_k$	Production rate of turbulence kinetic energy
$r$	Volume fraction
$R$	Radius of disc and cup
$\mathbf{u}$	Velocity vector

### Greek Symbols

$\alpha_3$	Constant in turbulence model
$\beta'$	Constant in turbulence model
$\beta_3$	Constant in turbulence model
$\varepsilon$	Dissipation rate of turbulence kinetic energy
$\kappa$	Local curvature of free surface
$\mu$	Dynamic viscosity
$\mu_t$	Turbulent viscosity
$\theta$	Taper angle of cup sidewall
$\rho$	Density
$\sigma_{\omega 2}$	Prandtl number for $\omega$ in transformed $k$ - $\varepsilon$ model
$\sigma_{\omega 3}$	Prandtl number for $\omega$ in SST turbulence model
$\sigma_{k3}$	Prandtl number for $k$ in SST turbulence model
$\omega$	Turbulence eddy frequency

### Subscripts

$\alpha$	Fluid phase identity (liquid slag or air)
$g$	Gas phase or gravitational force
$l$	Liquid phase
$s$	Surface tension force

The contributing editor for this article was Sharif Jahanshahi.

✉ Yuhua Pan  
ypan16@hotmail.com

<sup>1</sup> School of Materials and Metallurgy, University of Science and Technology Liaoning, 185 Qianshan Middle Road, Anshan 114051, Liaoning, China

## Introduction

Molten slags generated during pyrometallurgical production of metals are mostly treated as waste materials except that the blast furnace slag is utilized for cement production after water quenching treatment. The slags discharged from furnaces are in molten state with temperatures ranging from 1300 to 1650 °C and thus contain huge amount of heat energy. However, at present, this heat energy dissipates into atmosphere. In addition, almost all the slags, except ironmaking blast furnace slag, are currently disposed as landfill, polluting the environment. Only the blast furnace slag is nowadays mostly treated by water quenching (wet granulation) to produce a raw material for cement production, but most of the sensible heat of the slag is transferred to water to become a low-grade heat source (hot water), making the rich sensible heat resources in the molten slag not effectively utilized. In addition, wet granulation consumes large quantity of fresh water and emits toxic sulfur containing gases to the atmosphere. Therefore, it is high time that the heat energy in molten slags be recovered and all the slags be reused.

To reach the above-mentioned goal, heat recovery through atomizing molten slag without using water quenching, i.e., dry granulation, has become people's focus on developing new-generation technologies for slag treatment in the future. Consequently, various potential Dry Slag Granulation (DSG) technologies have emerged. According to literature review [1], since the 1970s, people have explored and developed a variety of DSG technologies to recover waste heat from molten slags, which can be generally classified into two types: centrifugal granulation by using, e.g., spinning disc/cup/drum and air blast quenching by using, e.g., air jet spray. Among them, centrifugal granulation technologies based on spinning discs and cups have received more attention and are considered to be superior to other granulation technologies because they possess the most potential to produce more uniform and fine slag particles that have large enough surface area-to-volume ratios ensuring fast cooling of the slag droplets and granules. Therefore, centrifugal granulation of molten slag likely becomes one of the most effective means to recover waste heat from slag in the future.

However, to date, the reported technologies of waste heat recovery from molten slag based on spinning disc and cup are still at the laboratory scale or pilot plant scale, and have not yet reached the scale of industrial production. The main reason is that the mechanism of centrifugal granulation of slag by spinning discs and cups has not been fully understood. Especially, the design and operation of the spinning discs and cups, as the core units of the technologies, have yet to be optimized through quantitative

analyses on influences of design and operating parameters on the size of slag granules produced, which is key to maintain smooth operation in large-scale industrial production process.

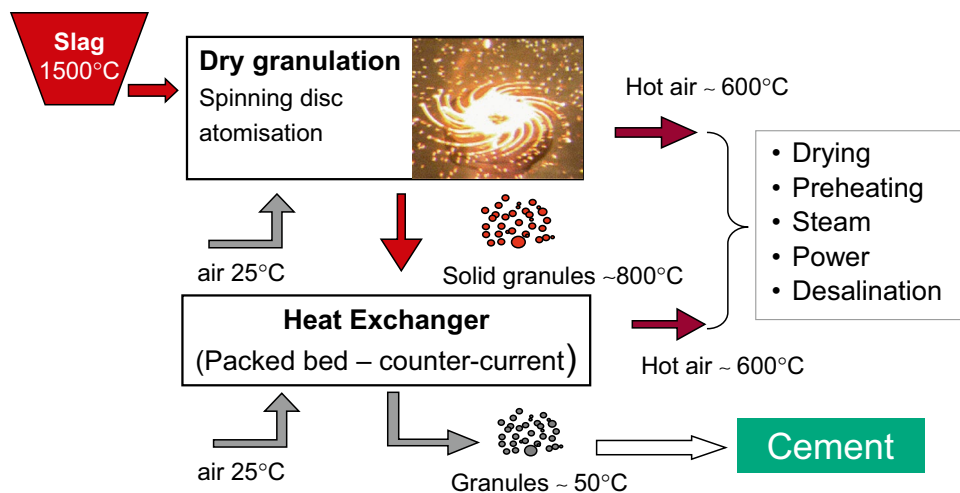
In this regard, the authors applied computational fluid dynamics (CFD) numerical modeling method to simulate the behavior of liquid slag flowing (spreading) on spinning discs and cups to predict the thickness of liquid slag film on the surface of the discs and cups. Especially, the liquid slag film thickness at the edge of the spinning discs and cups was predicted, and the effects of design and operating parameters for the discs and cups on the slag film thickness were examined. This is because the slag film thickness at the edge of the discs and cups has a predominant influence on the size of the droplets after the slag film breakup and hence that of the slag granules produced.

## Example of Technology of Centrifugal Granulation of Molten Slag with Heat Recovery

Figure 1 shows, as an example, a conceptual technology based on centrifugal granulation of molten blast furnace slag with heat recovery by using a spinning disc developed by Commonwealth Scientific and Industrial Research Organization (CSIRO) of Australia [2]. The slag discharged from the blast furnace (temperature at about 1500 °C) is poured onto the center of a disc that is spinning at a high speed inside a closely sealed container (called granulator). The centrifugal force imposed by the spinning disc drives the liquid slag to spread on the surface of the disc, forming a thin layer of slag film. On leaving the edge of the disc, the slag film first deforms into an array of liquid ligaments along the circumference of the disc that eventually break up into fine droplets. Cold air at room temperature (e.g., 25 °C) is blown into the granulator and quenches the molten slag droplets into solid granules and further cools the granules down to about 800 °C. Then, the slag granules are discharged from the granulator and fed into a countercurrent moving-bed heat exchanger. By introducing cold air at room temperature (also 25 °C, for instance), the hot slag granules are further cooled to a sufficiently low temperature (about 50 °C) that can be easily handled. The obtained slag granules have very high glass phase content and can be used as a raw material for cement production. Cold air introduced into both the granulator and the moving-bed heat exchanger can be heated by the hot slag into hot air of about 600 °C, which can find such applications as producing steam for power generation, drying or preheating materials, or desalination of seawater, etc.

The above-mentioned concept of DSG technology based on a spinning disc was first successfully demonstrated at CSIRO's Clayton laboratory on a pilot-scale 1.2-m diameter

**Fig. 1** Conceptual process flowsheet for integrated dry granulation and heat recovery [2] (Color figure online)



granulator processing molten slag at throughput rate of  $10 \text{ kg min}^{-1}$  [2], and then the technology was further scaled up to a present-day semi-industrial plant with 3 m diameter granulator that can process molten slag at throughput rate up to  $100 \text{ kg min}^{-1}$  (vs.  $6 \text{ t h}^{-1}$ ) [3]. The development of the DSG technology at CSIRO, current status, and future direction of the technology as well as its combination with other breaking-through technologies developed at CSIRO (e.g., technology of charcoal production through autogenous pyrolysis) as a potential solution for sustainable development of metallurgical industry were summarized by Jahanshahi et al. [4].

Nevertheless, one of the key issues in dry granulation of molten slag that still remains is how to produce slag granules with desired sizes that can facilitate fast heat exchange with air ensuring enough large cooling rate. As shown in Fig. 1, it can be seen that the thickness of liquid slag film at the edge of the disc directly affects the diameter of the liquid slag ligament formed, which further dominates the size of the slag droplets, i.e., the size of the solid slag granules after cooling to room temperature. Therefore, if one can know quantitatively the parameters influencing the thickness of the slag film at the disc edge, it will be to a large extent possible to effectively control the size of the solidified slag granules. However, in fact, the centrifugal granulation of molten slag is a complicated process involving high-temperature, multiphase, and high-speed flow with changing free surface topology, which makes it extremely difficult and even impossible to accurately measure the thickness of the slag film by experiments. Instead, in the present work, the authors apply a validated CFD model to predict the slag film thickness at the edge of the spinning disc and cup so as to find out quantitative relationship between the slag film thickness and the design and operating parameters such as size and shape of disc and cup and slag flowrate (feeding rate) and spinning speed of disc and cup.

## CFD Simulation on Centrifugal Granulation of Molten Slag

### Work Done So Far

With regard to the flow behavior of molten slag under centrifugal force imposed by spinning discs and cups, a number of CFD simulations have already been carried out by researchers in the past. Among them, Chen et al. [5] used Volume-of-Fluid (VOF) model in ANSYS Fluent software to establish a three-dimensional CFD model to simulate the process of granulating blast furnace slag with three types of concave rotary discs. They concluded that the second type of large rotary disc with deep concave cavity (15 mm in depth and 200 mm in diameter) was easier to break up molten slag into droplets. Wang et al. [6] also used the VOF model of ANSYS Fluent software to calculate the liquid slag film thickness distribution along the radius of a spinning disc with a special focus on the hydraulic jump formation on the disc. They found that the slag film thickness distribution is mainly determined by the volume flowrate and kinematic viscosity of molten slag as well as the rotational speed of the disc, and the hydraulic jump region is very small and has no effect on the slag flow after the hydraulic jump. Chang et al. [7] carried out experiments and CFD numerical simulations to study the spreading and granulation of molten blast furnace slag on smooth and rough spinning discs and suggested that discs with a smooth surface should be selected to produce fine slag particles and avoid slag wool formation. Using ANSYS CFX software, Pan et al. [8] performed two-dimensional multiphase flow simulations to study the behavior of molten blast furnace slag spreading on a flat disc, and then, by using the two-dimensional CFD model, Pan et al. [9] further performed numerical experiments using fractional factorial orthogonal design and investigated the influences of five parameters (liquid flowrate, disc spinning speed, disc radius, liquid viscosity, and density) on the

liquid film thickness at the disc edge. In addition, they also performed dimensional analysis on those parameters and, combined with the numerical simulation results, established a dimensionless relationship between the liquid film thickness and those parameters investigated, which could be applied to not only guide scale up of the centrifugal granulation technology but extend the technology to atomization of other types of liquid materials.

Most of the CFD simulations reported in literature are limited to the spreading process of molten slag on spinning discs with flat surface and few on spinning cups. Therefore, it is necessary to conduct a more systematic study on the effects of key parameters on the slag film thickness at the edge of spinning discs and cups. These include design parameters such as size and shape of the discs and cups and operating parameters such as feeding flowrate of the molten slag and spinning speed of the discs and cups. They form the main content of the present CFD modeling work and will be described in detail in the following sections.

## CFD Model Development

### Governing Equations

Under the assumptions of two-dimensional steady-state incompressible two-phase (liquid slag and air) turbulent flow and neglecting heat transfer, below are the partial differential equations governing the flow phenomena of interest to be numerically solved in the present modeling work:

Continuity equation:

$$\nabla \cdot (\rho \mathbf{u}) = 0. \quad (1)$$

Momentum equations:

$$\nabla \cdot (\rho \mathbf{u} \mathbf{u}) = -\nabla p + \nabla \cdot [(\mu + \mu_t)(\nabla \mathbf{u} + (\nabla \mathbf{u})^T)] + \mathbf{F}_g + \mathbf{F}_s. \quad (2)$$

Shear–Stress–Transport turbulence equations:

$$\nabla \cdot (\rho \mathbf{u} k) = \nabla \cdot \left[ \left( \mu + \frac{\mu_t}{\sigma_{k3}} \right) \nabla k \right] + P_k - \beta' \rho k \omega, \quad (3)$$

$$\nabla \cdot (\rho \mathbf{u} \omega) = \nabla \cdot \left[ \left( \mu + \frac{\mu_t}{\sigma_{\omega 3}} \right) \right] + (1 - F_1) 2\rho \frac{\nabla k \nabla \omega}{\sigma_{\omega 2} \omega} + \alpha_3 \frac{\omega}{k} P_k - \beta_3 \rho \omega^2. \quad (4)$$

Volume continuity equation:

$$\sum_{\alpha=1}^{N_p} \nabla \cdot (r_\alpha \mathbf{u}) = 0. \quad (5)$$

Volume conservation equation:

$$\sum_{\alpha=1}^{N_p} r_\alpha = 1. \quad (6)$$

In Eqs. (1) to (4), the fluid density  $\rho$  and viscosity  $\mu$  are defined, respectively, as

$$\rho = \sum_{\alpha=1}^{N_p} (r_\alpha \rho_\alpha), \quad (7)$$

$$\mu = \sum_{\alpha=1}^{N_p} (r_\alpha \mu_\alpha). \quad (8)$$

In Eq. (2),  $\mathbf{F}_g$  is the gravitational force and  $\mathbf{F}_s$  the body force due to liquid surface tension, which is approximately calculated by using the method of continuum surface force (CSF) reported by Brackbill et al. [10], and for liquid and gas, two-phase flows with a free surface  $\mathbf{F}_s$  can be calculated by Eq. (9):

$$\mathbf{F}_s = \frac{\sigma \kappa \rho \nabla r_l}{\frac{1}{2}(\rho_l + \rho_g)}. \quad (9)$$

Detailed meanings of the symbols used in Eqs. (1) to (9) are given in Nomenclature.

### Definitions of Computation Domain and Boundary Conditions

In the present modeling work, three types of spinning components for atomizing the liquid slag were investigated. They were flat surface disc, disc with a curved surface recess, and cup with different sidewall height and taper angle. Figure 2 shows computation domains and meshes as well as boundary condition types defined for these three types of spinning components.

As shown in Fig. 2, the left-hand side of the center axis of the spinning components is the computational domain with various types of boundaries defined. The length of the computation domains extends from the center axis of the spinning components to their edge (i.e., the radius  $R$ ), and its height extends to a certain distance above the spinning components to include a part of pouring slag stream. The right-hand side of the center axis is computation mesh defined for the corresponding computation domain. The computational mesh is comprised of non-uniform quadrilateral grids with sizes ranging from 0.025 mm to 1 mm. To resolve the thin film of liquid slag, the grid sizes less than 0.15 mm are concentrated in the vicinity of the surface of the discs and cups (see the enlarged mesh area in Fig. 2a, as an example). Tables 1 and 2 list the detailed boundary conditions defined

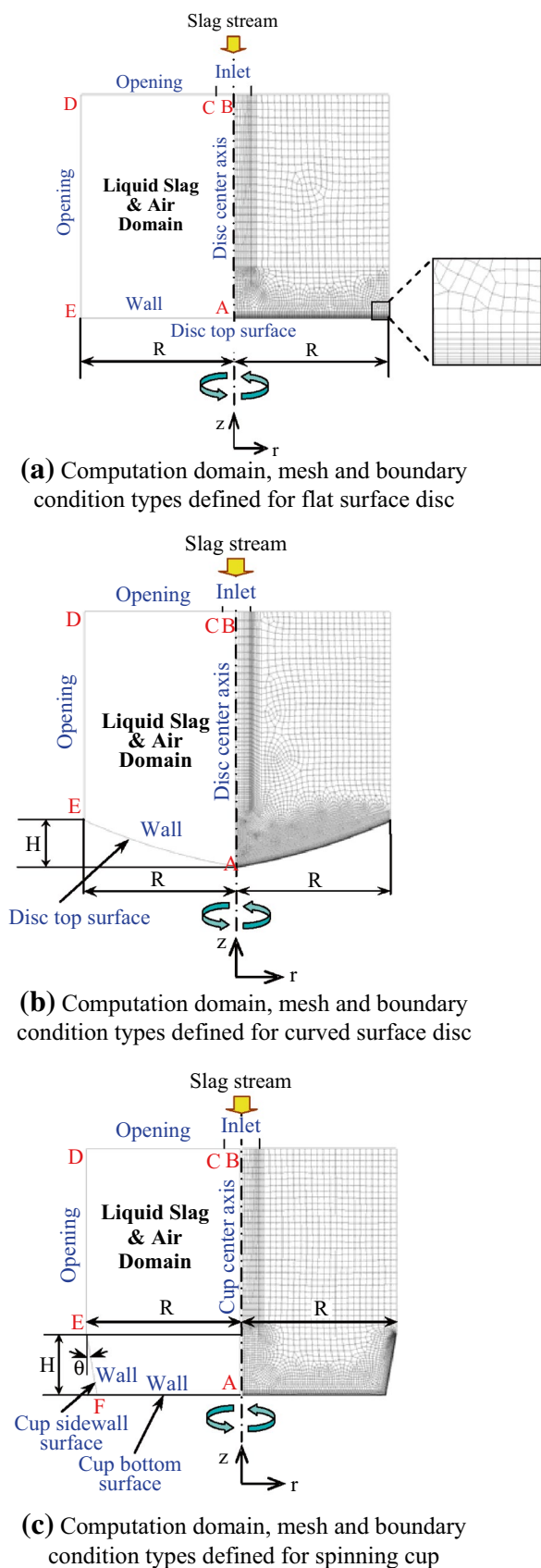


**Fig. 2** Computation domain, mesh, and boundary condition type (Color figure online)

in the CFD model (cf., Figure 2). And Table 3 gives the physical properties of the flow media (liquid blast furnace slag and air) used in the present numerical simulation study.

### Solution Method

CFD simulation software ANSYS CFX [12] was used to numerically solve the simultaneous governing Eqs. (1) to (6) to obtain the liquid slag and air two-phase flow field in the computation domains defined in Fig. 2. According to model predicted liquid slag and air interface (free surface) profile, the distribution of slag film thickness along the radial direction of the spinning components was determined and, thus, the thickness of the slag film at the spinning component edge was obtained.

## Results and Discussion

### Model Predicted Flow Field and Free Surface Profile

Figures 3, 4, and 5 show, respectively, model predicted flow fields and molten slag spreading phenomena on the surfaces of a flat disc, curved surface discs with different recess depth and inside spinning cups of different dimensions (cf., Fig. 2). These figures present the velocity vector field on the left-hand side of the center axis of the spinning components and the volume fraction field indicating free surface profile on the right-hand side. In the volume fraction fields, red area stands for molten slag region and blue area for air region, the interface between which, where the volume fraction equals to 0.5, is defined in the present work as free surface of liquid slag layer from which its thickness is obtained by visual measurement. It can be seen from these figures that under the action of centrifugal force, the slag quickly spreads to a thin liquid film on the surface of the spinning components. The velocity fields of slag and air indicate that larger velocity vectors are concentrated in the region of slag pouring stream (mainly driven by inlet flow and gravity) and inside the slag film and adjacent air (mainly driven by centrifugal force).

The slag film thickness at the edge of the spinning components is defined as the vertical distance from the edge to the free surface (i.e., iso-surface at liquid slag volume fraction of 0.5) according to the model predicted free surface profile. As mentioned before, this film thickness is an important parameter that could dominate the size of the slag droplets and particles produced by the centrifugal granulation techniques. Thus, in the present modeling work, we investigated the effects of such factors as the design parameters ( $H$  and  $\theta$ , cf., Fig. 2) of the spinning components and operating parameters (slag flowrate and spinning speed) on the slag film thickness at the edge of



**Table 1** Boundary conditions defined for discs with flat and curved surfaces (cf., Fig. 2a and b)

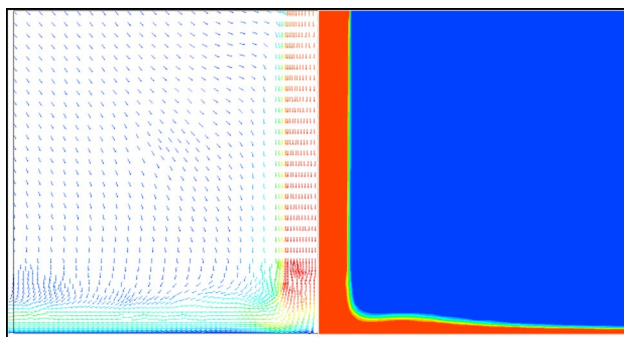
Boundary	Boundary name	Boundary type	Condition
AB	Center axis	Rotating symmetrical axis	Zero flux
BC	Liquid slag inlet	Inlet	Fixed mass flowrate ( $\text{kg s}^{-1}$ )
CD	Top boundary	Opening	Fixed pressure ( $=0 \text{ Pa}$ )
DE	Side boundary	Opening	Fixed pressure ( $=0 \text{ Pa}$ )
EA	Disc top surface	Wall	Non-slip rotating wall

**Table 2** Boundary conditions defined for spinning cups (cf., Fig. 2c)

Boundary	Boundary name	Boundary type	Condition
AB	Center axis	Rotating symmetrical axis	Zero flux
BC	Liquid slag inlet	Inlet	Fixed mass flowrate ( $\text{kg s}^{-1}$ )
CD	Top boundary	Opening	Fixed pressure ( $=0 \text{ Pa}$ )
DE	Side boundary	Opening	Fixed pressure ( $=0 \text{ Pa}$ )
EF	Cup sidewall surface	Wall	Non-slip rotating wall
FA	Cup bottom surface	Wall	Non-slip rotating wall

**Table 3** Physical properties of molten blast furnace slag and air used in CFD model

Material	Density ( $\text{kg m}^{-3}$ )	Dynamic viscosity (Pa s)	Surface tension ( $\text{N m}^{-1}$ )	Reference
Liquid slag	2590	0.5	0.478	[11]
Air (at 25 °C)	1.185	$1.831 \times 10^{-5}$	–	[12]

**Fig. 3** Example of model predicted flow field (left) and volume fraction field (right) showing free surface profile (red color: liquid slag, blue color: air) above the flat surface disc (Conditions: Slag flowrate =  $5 \text{ kg min}^{-1}$ , Spinning speed = 1500 RPM,  $R=25 \text{ mm}$ , cf., Fig. 2a) (Color figure online)

those spinning components, and the results are provided and discussed in the following sections.

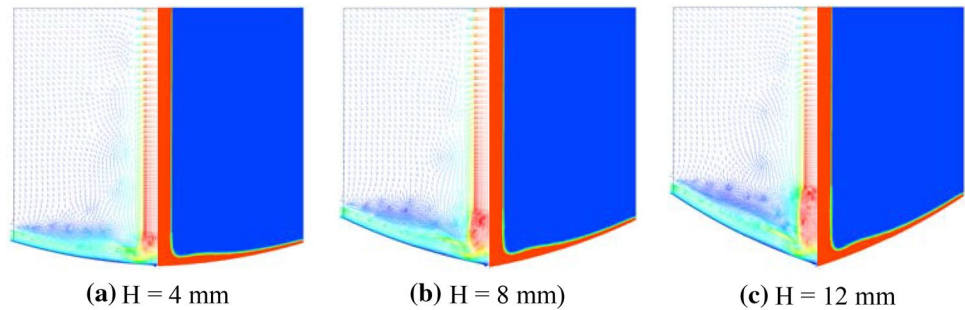
### Effects of Design and Operating Parameters on Slag Film Thickness

Figure 6 shows the model predicted slag film thickness as functions of slag flowrate and spinning speed for different

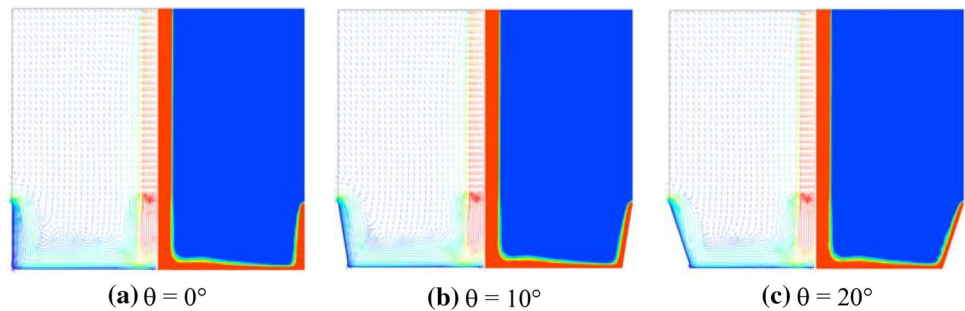
types of the spinning components of the same size (radius). It can be seen from this figure that the slag film thickness increases with the increase of the slag flowrate (Fig. 6a) but decreases at higher spinning speed (Fig. 6b). Figure 6 also depicts that, among the three types of the spinning components investigated, the flat surface disc produces the thickest slag film followed by the spinning cup, whereas the curved surface disc makes the slag film thinnest. For the same radius ( $R$ ) and operating conditions, liquid slag has a larger contact (wetting) area with the surfaces of spinning cup and curved surface disc than the flat surface disc and thus spreads into thinner films than the latter. Furthermore, compared with the spinning cup, the slag film thickness at the curved surface disc edge is smaller than that on the cup edge. The reason is that the cup has a sharp corner and a sidewall that impose a larger resistance to the slag flow, whereas the curved surface disc has a smooth surface that exerts a smaller resistance to the slag flow.

For spinning components with a recess like spinning cups and curved surface discs, the effects of their design parameters like recess depth ( $H$ ) and cup sidewall taper angle ( $\theta$ ), cf., Fig. 2, on the slag film thickness were also studied in the present work and the modeling results are illustrated in Fig. 7. As shown in Fig. 7a, the characteristics of the influence of  $H$  on the slag film thickness is rather different between the spinning cup and the curved surface disc. The slag film thickness increases with  $H$  of the cup but decrease with  $H$  of the curved surface disc. This is because the cup's sidewall blocks the slag flow and thus makes it form a thicker layer before leaving the edge of the cup, while the curved surface disc has a smooth surface but its area becomes larger as  $H$  increases, i.e., a larger wetting area, so that the slag film at the disc edge becomes thinner. Figure 7b shows that on spinning cups when its sidewall taper angle  $\theta$  increases, the

**Fig. 4** Examples of model predicted flow field (left) and volume fraction field (right) showing free surface profile (red color: liquid slag, blue color: air) above the curved surface discs (Conditions: Slag flowrate =  $5 \text{ kg min}^{-1}$ , Spinning speed = 1500 RPM,  $R = 25 \text{ mm}$ , cf., Fig. 2b) (Color figure online)



**Fig. 5** Examples of model predicted flow field (left) and volume fraction field (right) showing free surface profile (red color: liquid slag, blue color: air) inside spinning cups (Conditions: Slag flowrate =  $5 \text{ kg min}^{-1}$ , Spinning speed = 1500 RPM,  $R = 25 \text{ mm}$ ,  $H = 10 \text{ mm}$ , cf., Fig. 2c) (Color figure online)



slag film thickness tends to decrease. When  $\theta = 0^\circ$ , which corresponds to a vertical sidewall, the sidewall imposes the largest resistance to the slag flow and thus makes the slag layer thicker; as  $\theta$  increases, i.e., the sidewall becomes more inclined, the sidewall has a less resistance to the slag flow and consequently the slag film becomes thinner.

## Conclusions

In the present work, the liquid slag film thickness at the edge of three types of spinning components (flat surface disc, curved surface discs, and cups) was predicted by performing CFD model simulations, and the effects of the shape

of the discs and cups and the operating parameters on the slag film thickness were examined. The follow conclusions can be drawn:

- The slag film thickness increases with the increase of the slag flowrate and decreases with the increase of the spinning speed.
- Under the same slag flowrate and spinning speed, the larger the wetting area of the liquid slag on the discs and cups, the smaller the slag film thickness. Thus, for the same radius ( $R$ ), the slag film thickness on the flat surface disc having smaller wetting area is larger than those on curved surface disc and cup with larger wetting areas.

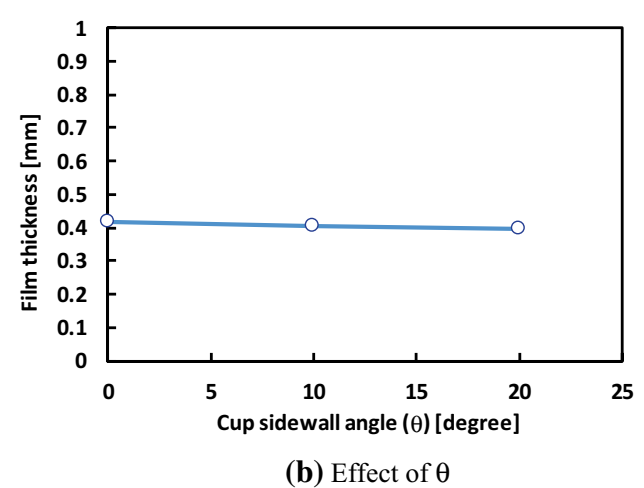
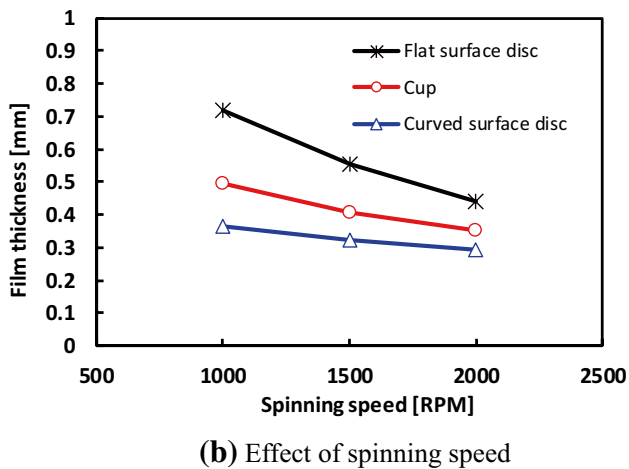
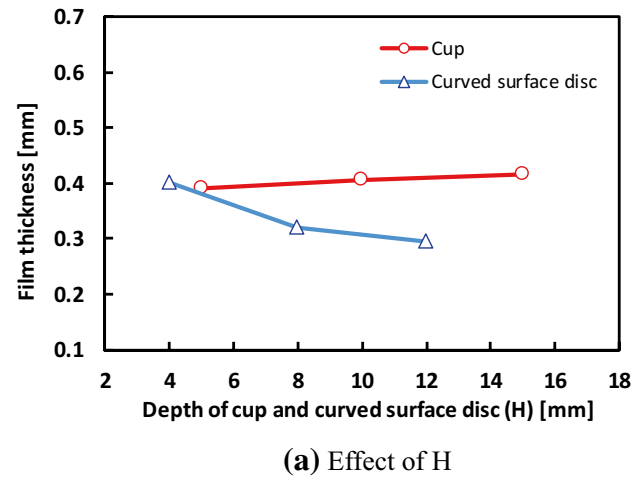
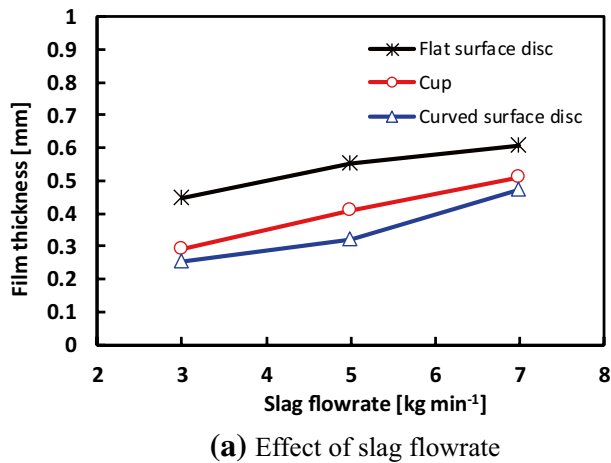


**Fig. 6** Predicted slag film thickness as functions of slag flowrate and spinning speed for different types of spinning components (Conditions: Slag flowrate=5 kg min<sup>-1</sup>, Spinning speed=1500 RPM,  $R=25$  mm,  $H=10$  mm, and  $\theta=10^\circ$ , cf., Fig. 2) (Color figure online)

**Fig. 7** Predicted slag film thickness as functions of recess depth ( $H$ ) and sidewall angle of ( $\theta$ ) cup (Conditions: Slag flowrate=5 kg min<sup>-1</sup>, Spinning speed=1500 RPM,  $R=25$  mm, cf., Fig. 2c) (Color figure online)

- For the same radius ( $R$ ), the spinning cup has sharp corner between bottom and sidewall that imposes a larger resistance to the slag flow and thus the slag film thickness on the cup edge is larger than that on the curved surface disc, which has a smooth surface that exerts a smaller resistance to the slag flow.
- The slag film thickness increases with the recess depth ( $H$ ) of the cup, as the higher the cup's sidewall, the

- larger the resistance to the slag flow and hence forming a thicker slag layer at the edge of the cup.
- The slag film thickness decreases with the recess depth ( $H$ ) of the curved surface disc, since the curved surface disc has a smooth surface but its area is larger when the recess goes deeper, i.e., a larger wetting area, so that the slag film at the disc edge becomes thinner.
- When the spinning cup sidewall taper angle ( $\theta$ ) increases, the slag film thickness tends to decrease due to a less resistance of the sidewall to the slag flow and consequently the slag film becomes thinner.



**Acknowledgements** The present work was financially supported by Education Department of Liaoning Province (Grant No.: 2017LNQN17), China, and University of Science and Technology Liaoning (Grant No.: 2016QN19), China.

## References

1. Barati M, Esfahani S, Utigard TA (2011) Energy recovery from high temperature slags. *Energy* 36:5440–5449
2. Jahanshahi S, Xie D, Pan Y, Ridgeway P, Mathieson JG (2011) Dry slag granulation with integrated heat recovery. 1st International conference on energy efficiency and CO<sub>2</sub> reduction in the steel industry (EECR Steel 2011)—incorporated in METEC InSteelCon 2011, 27 June–1 July, Dusseldorf, Germany, pp. Session 13 (p 7)
3. Jahanshahi S, Pan Y, Xie D (2012) Some fundamental aspects of dry slag granulation process. In: 9th International Conference on Molten Slags, Fluxes and Salts (Molten12), Beijing, 27–31 May 2012, CD-ROM
4. Jahanshahi S, Mathieson JG, Somerville MA, Haque N, Norgate TE, Deev A, Pan Y, Xie D, Ridgeway P, Zulli P (2015) Development of low-emission integrated steelmaking process. *J Sustain Metall* 1:94–114. <https://doi.org/10.1007/s40831-015-0008-6>
5. Chen Y, Ma J, Zhao H, Yang G (2013) Numerical simulation and experimental study on centrifugal atomization about blast furnace slag. *Comput Simul* 30(2):235–238, 273 (In Chinese)
6. Wang D, Ling X, Peng P (2014) Theoretical analysis of free-surface film flow on the rotary granulating disk in waste heat recovery process of molten slag. *Appl Therm Eng* 63:387–395
7. Chang Q, Li X, Ni H, Zhu W, Pan C, Hu S (2015) Modeling on dry centrifugal granulation process of molten blast furnace slag. *ISIJ Int* 55(7):1361–1366
8. Pan Y, Witt PJ, Xie D (2010) CFD simulation of free surface flow and heat transfer of liquid slag on a spinning disc for a novel dry slag granulation process. *Prog Comput Fluid Dyn* 5(6):292–299
9. Pan Y, Witt PJ, Kuan B, Xie D (2014) CFD modelling of the effect of operating parameters on the spreading of liquids on a spinning disc. *J Comput Multiph Flow* 6(1):49–64
10. Brackbill JU, Kothe DB, Zemach C (1992) A continuum method for modelling surface tension. *J. Comput Phys* 100:335–354
11. Inaba S, Kimura Y, Shibata H, Ohta H (2004) Measurement of physical properties of slag formed around the raceway in the working blast furnace. *ISIJ Int* 44(12):2120–2126
12. ANSYS Inc., ANSYS CFX user's manual

**Publisher's Note** Springer Nature remains neutral with regard to jurisdictional claims in published maps and institutional affiliations.